

Optimizing Thermodynamic Cycles with Two Finite-Sized Reservoirs

Hong Yuan,¹ Yu-Han Ma,^{1,*} and C. P. Sun^{1,2,†}

¹Graduate School of China Academy of Engineering Physics,
No. 10 Xibeiwang East Road, Haidian District, Beijing, 100193, China
²Beijing Computational Science Research Center, Beijing 100193, China

We study the non-equilibrium thermodynamics of a heat engine operating between two finite-sized reservoirs with well-defined temperatures. Within the linear response regime, it is discovered that there exists a power-efficiency trade-off depending on the ratio of heat capacities (γ) of the reservoirs for the engine; the uniform temperature of the two reservoirs at final time τ is bounded from below by the entropy production $\sigma_{\min} \propto 1/\tau$. We further obtain a universal efficiency at maximum power of the engine for arbitrary γ . Our findings can be used to develop an optimization scenario for thermodynamic cycles with finite-sized reservoirs in practice.

Introduction.—The thermodynamic constraints exist in all kinds of energy-conversion machines. Among these constraints, Carnot efficiency serves as the upper bound of the efficiency of heat engines, which is only achieved by reversible thermodynamic cycles with sufficiently long operation time [1]. In this sense, the reversible heat engines have vanishing output power and thus are valueless in practice. For practical purposes, extensive studies on finite-time thermodynamic cycles have been carried out by considering the restriction on operation time over the past decades [2–6]. Abundant thermodynamic constraints for heat engines were discovered successively [6], such as, efficiency at maximum power (EMP) [7–17], trade-off relation between power and efficiency [18–23], and thermodynamic uncertainty relation (TUR) [24, 25]. It was recognized that these finite-time constraints are primarily caused by the energy dissipation in the irreversible thermodynamic cycles. Especially, the power-efficiency trade-off has attracted considerable attention since it predicts the feasible operation regime for practical heat engines.

Recently, the finiteness of the reservoir size is taken into account as another practical restriction on thermodynamic cycles since the heat is basically stored by a finite amount of material with finite heat capacity [26–33]. The heat engines operating between two finite-sized reservoirs will eventually stop operating when the reservoirs reach the final thermal equilibrium state with a uniform temperature depending on the ratio of heat capacities of the reservoirs. In this case, the efficiency at maximum work (EMW) [26, 28, 33, 34] and efficiency at maximum average power (EMAP) [27, 29, 30, 33] were proposed as typical thermodynamic constraints.

In essence, both the finiteness of operation time and reservoir size result in thermodynamic constraints on heat engines by influencing their power and efficiency. Usually, these two restrictions appear jointly in the real-world circumstances. Hence, a more practical question arises whether a power-efficiency trade-off exists in the

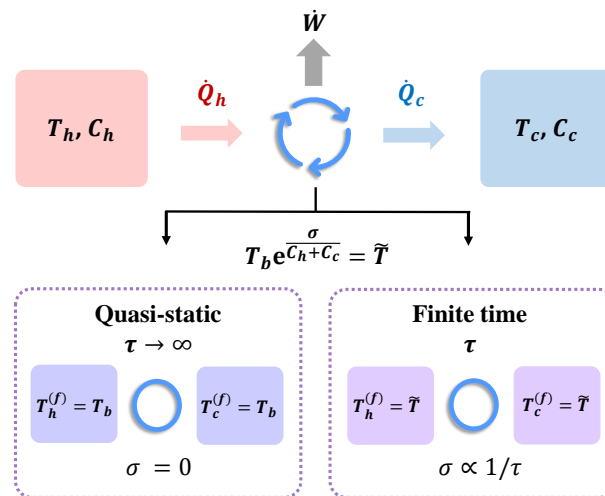


Figure 1. Demonstration of a heat engine operating between two finite-sized heat reservoirs. The heat engine operates between a finite-sized hot (cold) reservoir with initial temperature $T_h^{(i)}$ ($T_c^{(i)}$). The heat engine stops working when the two reservoirs reach a the final uniform temperature $T_c^{(f)} = T_h^{(f)} \equiv \tilde{T}$. C_c (C_h) denotes the heat capacity of the cold (hot) reservoir. Due to the entropy production of the thermodynamic cycle in finite time operation, $\tilde{T} > T_b$ [Eq. (2)].

case with finite-sized reservoirs, which is crucial for developing a unified optimization theory for practical heat engines. In this Letter, we address this question by studying the finite-time performance of a linear irreversible heat engine operating between two finite-sized reservoirs. With the discovered trade-off relation, we further find a universal EMAP which is applicable to the case with arbitrary ratio of heat capacities of the reservoirs.

The minimum entropy production and the uniform temperature.— As illustrated in Fig. 1, we consider a linear irreversible heat engine operating between a hot reservoir with initial temperature $T_h^{(i)}$ and a cold reservoir with initial temperature $T_c^{(i)}$. Both of these two reservoirs are of finite size with the heat capacity C_h and C_c , respectively. As follows, we focus on the case of constant

* yhma@gscaep.ac.cn

† suncp@gscaep.ac.cn

heat capacity $C_{h(c)}$. The engine converts the heat to work consecutively until the two reservoirs finally reach the thermal equilibrium state with the uniform temperature $T_c^{(f)} = T_h^{(f)} \equiv \tilde{T}$, and the operation time of the whole process is denoted as τ . Here, we have implicitly assumed that the heat capacity of at least one reservoir is finite, otherwise the temperature of the two reservoirs will always maintain their initial values instead of reaching the same. In the following, we adopt the assumptions used in the Refs. [29, 30, 33]: (i) both of the two reservoirs relax rapidly such that they are always in the quasi-equilibrium states with time-dependent temperatures, $T_h(t)$ for the hot reservoir and $T_c(t)$ for the cold one. Correspondingly, the initial and final conditions are $T_\alpha(0) = T_\alpha^{(i)}$ and $T_\alpha(\tau) = T_\alpha^{(f)}$ ($\alpha = h, c$), respectively; (ii) the total operation time τ is much larger than the cycle time τ_c (unit time), and hence the engine undergoes sufficiently many cycles before it stops operating.

The entropy production rate reads $\dot{\sigma} = -\dot{Q}_h/T_h + \dot{Q}_c/T_c$, where $\dot{Q}_h = -C_h\dot{T}_h$ is the heat flow from the hot reservoir to the engine, and $\dot{Q}_c = C_c\dot{T}_c$ is the heat flow from the engine to the cold reservoir. As a result, the total entropy production $\sigma(\tau) \equiv \int_0^\tau \dot{\sigma} dt$ in the whole process is

$$\sigma(\tau) = C_c \ln \frac{\tilde{T}}{T_c^{(i)}} + C_h \ln \frac{\tilde{T}}{T_h^{(i)}}. \quad (1)$$

The final temperature \tilde{T} is thus determined by the entropy production $\sigma = \sigma(\tau)$ as

$$\tilde{T} = \tilde{T}(\sigma) = \left[T_h^{(i)} \right]^{\frac{1}{\gamma+1}} \left[T_c^{(i)} \right]^{\frac{\gamma}{\gamma+1}} \exp \left[\frac{\sigma}{C_h + C_c} \right], \quad (2)$$

which indicates that the final temperature rises as the entropy production increases. Here $\gamma \equiv C_c/C_h$, being the heat capacity ratio, quantifies the asymmetry in size of the two reservoirs. $T_b \equiv \tilde{T}(\sigma = 0)$ is the final temperature in the reversible case with no entropy production. The detailed discussion about the reversible case is illustrated in the Supplementary Materials (SM) [35].

Then, we employ the linear irreversible thermodynamics to obtain $\sigma(\tau)$ as well as \tilde{T} explicitly in the finite-time regime. Under the tight-coupling condition, the entropy production rate reads [29, 30]

$$\dot{\sigma} = \frac{C_h^2 \dot{T}_h^2}{L_{22}}, \quad (3)$$

where the Onsager coefficient L_{22} corresponds to the thermal conductivity which relies on detailed heat transfer models for different physical systems [36–38]. The Cauchy-Schwarz inequality

$$\left[\int_0^\tau (\sqrt{\dot{\sigma}})^2 dt \right] \left(\int_0^\tau dt \right) \geq \left(\int_0^\tau \sqrt{\dot{\sigma}} dt \right)^2 \quad (4)$$

implies that the entropy production $\sigma(\tau) = \int_0^\tau \dot{\sigma} dt = \int_0^\tau (\sqrt{\dot{\sigma}})^2 dt$ has a lower bound, namely, [35]

$$\sigma(\tau) \geq \frac{\Sigma_{\min}}{\tau} \equiv \sigma_{\min}. \quad (5)$$

Here, only the first order of τ^{-1} is kept in the linear irreversible regime [16]. The minimum dissipation coefficient $\Sigma_{\min} \equiv (\int_{T_h^{(i)}}^{T_b} C_h dT_h / \sqrt{L_{22}})^2$, characterizing how irreversible entropy production increases away from the reversible regime, is a τ -independent dissipation coefficient. Generally, Σ_{\min} depends on the specific form of L_{22} and relates to the thermodynamic length [38–41]. In the simplest case with constant L_{22} , $\Sigma_{\min} = C_h^2 [T_h^{(i)} - T_b]^2 / L_{22}$. Besides, it is worth mentioning that the $1/\tau$ -scaling of irreversible entropy production shown in Eq. (5) is also discovered in the slow-driving finite-time isothermal processes [15, 23, 42, 43]. It follows from Eqs. (2) and (5) that the final temperature \tilde{T} is bounded from below by the minimal entropy production as $\tilde{T} = \tilde{T}(\sigma) \geq \tilde{T}(\sigma_{\min})$. Next, we will show that the increase in the final temperature will lead to less work output.

Trade-off between power and efficiency– In the entire process with duration τ , according to the law of energy conservation, the work output is $W(\tau) = Q_h(\tau) - Q_c(\tau)$. Here $Q_h(\tau) = C_h [T_h^{(i)} - \tilde{T}]$ and $Q_c(\tau) = C_c [\tilde{T} - T_c^{(i)}]$. The maximum extractable work is achieved under the reversible regime with no entropy production, namely $W_{\max} \equiv \lim_{\sigma \rightarrow 0} W(\tau)$ [35]. Note that $W(\tau)$ is a monotonically decreasing function of \tilde{T} [35], which indicates that, referring to Eq. (2), the entropy production will reduce $W(\tau)$ in comparison with W_{\max} . In this sense, we define the finite-time dissipation work $W_d = W_d(\tau)$ as

$$W_d \equiv W_{\max} - W(\tau) = (C_h + C_c) (\tilde{T} - T_b). \quad (6)$$

It follows from Eqs. (2), (5), and (6) that the constraint on dissipation work is explicitly obtained as $W_d \geq T_b \Sigma_{\min} / \tau \equiv W_d^{(\min)}$ [35]. In terms of W_d , the efficiency in the finite-time case, $\eta = \eta(\tau) \equiv W(\tau) / Q_h(\tau)$, reads

$$\eta = \frac{W_{\max} - W_d}{W_{\max} / \eta_{\text{MW}} - W_d / (1 + \gamma)}, \quad (7)$$

where the efficiency at maximum work (EMW) [35]

$$\eta_{\text{MW}} \equiv 1 - \gamma \left[\frac{\eta_C}{1 - (1 - \eta_C)^{\gamma/(\gamma+1)}} - 1 \right] \quad (8)$$

is achieved in the reversible regime [33], and $\eta_C \equiv 1 - T_c^{(i)} / T_h^{(i)}$ is the Carnot efficiency determined by the initial temperatures of the two reservoirs.

W_d can be expressed in terms of η according to Eq. (7), and then the constraint on dissipation work, namely, $W_d \geq W_d^{(\min)}$, becomes,

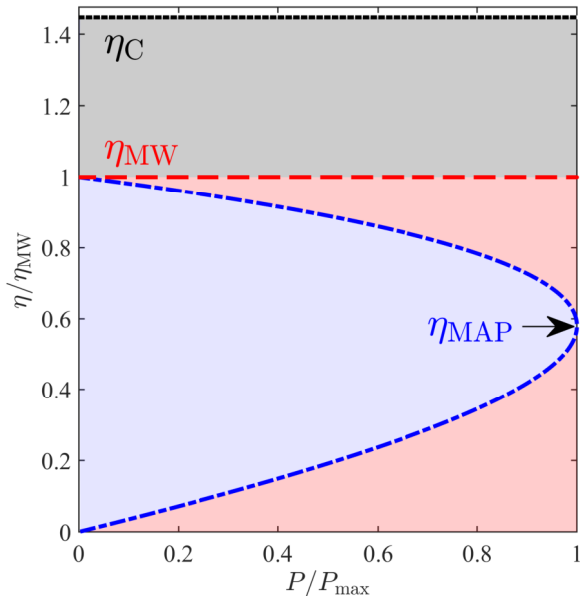


Figure 2. "Phase diagram" $\tilde{P} - \tilde{\eta}$ of the heat engine performance between finite reservoirs. The blue dash-dotted curve and the (light blue) area therein represent the trade-off between $\tilde{P} = P/P_{\max}$ and $\tilde{\eta} = \eta/\eta_{\text{MW}}$ in Eq. (10). P_{\max} here is the maximum average power. The efficiency at maximum work η_{MW} in Eq. (8) is plotted with the red dashed line, while the corresponding Carnot efficiency $\eta_{\text{C}} = 0.8$ is plotted with the black dotted line. In this example, we choose $\gamma = C_c/C_h = 1$.

$$W_d = \frac{W_{\max} (\eta_{\text{MW}} - \eta)}{\eta_{\text{MW}} [1 - \eta/(1 + \gamma)]} \geq \frac{T_b \Sigma_{\min}}{\tau}. \quad (9)$$

Eliminating the duration τ in this inequality with the average power $P \equiv W(\tau)/\tau$ of the whole process, we obtain the trade-off between power and efficiency as [35]

$$\tilde{P} \leq \frac{4\lambda\tilde{\eta}(1 - \tilde{\eta})}{(\lambda\tilde{\eta} + 1 - \tilde{\eta})^2}. \quad (10)$$

Here, $\lambda \equiv 1 - \eta_{\text{MW}}/(1 + \gamma)$, $\tilde{P} \equiv P/P_{\max}$, $\tilde{\eta} \equiv \eta/\eta_{\text{MW}}$, and $P_{\max} = W_{\max}/(2\tau^*)$ is the maximum average power achieved at $\tau = \tau^* \equiv 2T_b \Sigma_{\min}/W_{\max}$. As the main result of this paper, the above relation specifies the complete optimization regime for the heat engines operating between finite-sized reservoirs. In the symmetric case with $\gamma = 1$, such a trade-off is illustrated in Fig. 2 with the blue dash-dotted curve and the (light blue) area therein. The efficiency corresponding to the maximum power ($\tilde{P} = 1$) is denoted as η_{MAP} in this figure, and will be detailed discussed in the following. In this plot, $\eta_{\text{C}} = 0.8$ is used (See SM [35] for the asymmetric cases with $\gamma = 0.01, 100$). Due to the finiteness of the heat reservoirs, the (gray) area between efficiency at maximum work η_{MW} (red dashed line) and Carnot efficiency

η_{C} (black dotted line) becomes a forbidden regime in the "phase diagram" of the heat engine performance. Particularly, in the limit of $\gamma \rightarrow \infty$ with infinite cold reservoir, the trade-off in Eq. (10) reduces to a concise form $\tilde{P} \leq 4\tilde{\eta}(1 - \tilde{\eta})$.

With the power-efficiency trade-off in Eq. (10), it is straightforward to find the efficiency at an arbitrary given power \tilde{P} being bounded in the region of $\tilde{\eta}_- \leq \tilde{\eta} \leq \tilde{\eta}_+$, where $\tilde{\eta}_{\pm}$ are defined as [35]

$$\tilde{\eta}_{\pm} \equiv 1 - \frac{\lambda\tilde{P}}{(1 \pm \sqrt{1 - \tilde{P}})^2 + \lambda\tilde{P}}. \quad (11)$$

The upper bound $\tilde{\eta}_+$, serving as the maximum efficiency for an arbitrary average power, returns to its counterpart in the infinite-reservoir case by replacing η_{MW} with η_{C} [19, 20, 23]. Obviously, $\tilde{\eta}_+$ approaches 1 in the quasi-static regime of $\tilde{P} \rightarrow 0$, namely, $\eta \rightarrow \eta_{\text{MW}}$, as shown in Fig. 2. On the other hand, when $\tilde{P} \rightarrow 1$, the efficiency at maximum average power (η_{MAP}) is achieved. Below, we will further discuss η_{MAP} in detail.

Efficiency at maximum average power– In the maximum average power regime of $\tilde{P} = 1$, both of the upper bound and lower bound in Eq. (11) converge to the efficiency at maximum average power (EMAP) [35], namely,

$$\eta_{\text{MAP}} \equiv \tilde{\eta}_{\pm} (\tilde{P} = 1) = \frac{\eta_{\text{MW}}}{2 - \eta_{\text{MW}}/(1 + \gamma)}. \quad (12)$$

Since the heat capacity ratio $\gamma \in [0, \infty]$, η_{MAP} satisfies the following inequality

$$\eta_{\text{L}} \equiv \frac{\eta_{\text{MW}}}{2} \leq \eta_{\text{MAP}} \leq \frac{\eta_{\text{MW}}}{2 - \eta_{\text{MW}}} \equiv \eta_{\text{U}}, \quad (13)$$

where the upper (lower) bound η_{U} (η_{L}) is reached in the limit $\gamma \rightarrow 0$ ($C_c \ll C_h$) [$\gamma \rightarrow \infty$ ($C_c \gg C_h$)]. It is worth emphasizing here that the result related to an infinite large cold reservoir with $\gamma \rightarrow \infty$, i.e., $\eta_{\text{L}} = \eta_{\text{MW}}/2$ is the same as that obtained by Izumida and Okuda [29]. However, in contradiction with the expectation of Ref. [29] that $\eta_{\text{MW}}/2$ serves as the *upper bound* for η_{MAP} , our general result in Eq. (13) shows that $\eta_{\text{MW}}/2$ is actually the *lower bound* for η_{MAP} . The correct upper bound $\eta_{\text{U}} = \eta_{\text{MW}}/(2 - \eta_{\text{MW}})$ can surpass $\eta_{\text{MW}}/2$ to a greater extent with large η_{MW} .

Figure 3(a) shows the dependence of η_{MAP} on η_{C} , where the (light red) area between η_{U} (red dash-dotted curve) and η_{L} (red dotted curve) is the available range of η_{MAP} . In comparison, the achievable range of η_{MW} is represented with the (gray) area between the black solid curve and the black dashed curve. As demonstrated in this figure, in the small- η_{C} regime, there exist γ -independent scalings for η_{MAP} and η_{MW} . Such universalities can be explicitly obtained by expanding η_{MAP} and η_{MW} with respect to η_{C} :

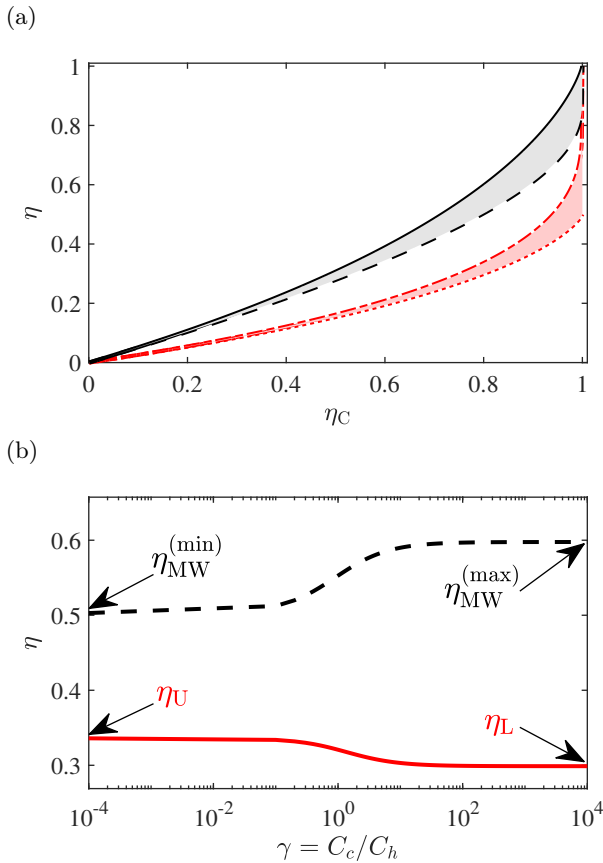


Figure 3. Dependence of η_{MAP} and η_{MW} on η_C and γ . (a) η_{MAP} and η_{MW} as the function of η_C . The upper (lower) bound η_U (η_L) of η_{MAP} in Eq. (13) is plotted as the red dash-dotted (dotted) curve, the (light red) area between the dash-dotted curve and dotted curve is the available range of η_{MAP} . The upper (lower) bound of η_{MW} is represented by the black solid (dashed) curve, and the (gray) area between the solid curve and dashed curve is the achievable range of η_{MW} . (b) η_{MAP} and η_{MW} as the function of γ . The red solid curve and black dashed curve represent η_{MAP} and η_{MW} , respectively. In this example, $\eta_C = 0.8$.

$$\eta_{MW} = \frac{1}{2}\eta_C + \frac{1}{6}\left(1 - \frac{1/2}{\gamma+1}\right)\eta_C^2 + \mathcal{O}(\eta_C^3) \quad (14)$$

$$\eta_{MAP} = \frac{1}{4}\eta_C + \frac{1}{12}\left(1 + \frac{1/4}{\gamma+1}\right)\eta_C^2 + \mathcal{O}(\eta_C^3) \quad (15)$$

We see that the first-order coefficients of both η_{MW} and η_{MAP} are independent of the heat capacity ratio γ , as we inferred from Fig. 3(a). Up to the first order of η_C , the universality for η_{MAP} is $\eta_{MAP} \sim \eta_C/4$. Meanwhile, the universality for η_{MW} behaves as $\eta_{MW} \sim \eta_C/2$, which has been reported in our previous study [33]. Nevertheless, the coefficients corresponding to the second order

of η_C are γ -dependent for η_{MAP} and η_{MW} . The signs of the terms containing γ in η_{MAP} and η_{MW} are opposite, which indicates that the monotonicity of η_{MAP} and η_{MW} with respect to γ is opposite. This fact is clearly illustrated in Fig. 3(b), where η_{MAP} (red solid curve) is a monotonically decreasing function of γ , while η_{MW} (black dashed curve) increases with γ monotonically. In this figure, the maximum η_{MW} ($\eta_{MW}^{(max)}$) and minimum η_{MW} ($\eta_{MW}^{(min)}$) are reached in the limit $\gamma \rightarrow \infty$ and $\gamma \rightarrow 0$, respectively [33], and $\eta_C = 0.8$ is fixed. As the result of the opposite monotonicity, there exists a competitive relation between η_{MAP} and η_{MW} . Namely, η_{MAP} achieves its maximum even when η_{MW} is minimum in the limit $\gamma \rightarrow 0$, and vice versa. It should be noted that, as the counterparts of η_{MAP} and η_{MW} in the infinite reservoir case, efficiency at maximum power (η_{MP}) and Carnot efficiency (η_C) have the same monotonicity with respect to the ratio of temperatures of the reservoirs.

Conclusion and discussion—In summary, we successfully obtained the power-efficiency trade-off for a linear irreversible heat engine operating between two finite-sized reservoirs. With such a trade-off, we showed the achievable range of efficiency for a given average power, which gives the universal efficiency at maximum average power. Moreover, by replacing η_{MW} with η_C , some typical constraints in finite case, such as efficiency at maximum power and maximum efficiency at arbitrary power, become their corresponding counterparts in infinite case. These thermodynamic constraints specific the full operation regime of the heat engines in real-world circumstances, and pave the way for the joint optimization of thermodynamic cycle by adjusting the ratio of the heat capacities of the reservoirs and controlling the operation of the cycle. Basically, this work sheds new light on investigating the irreversibility of non-equilibrium thermodynamic processes off thermodynamic limit. The predicted results can be tested on some state-of-art platforms, such as trapped Brownian particle [44].

However, as the quasi-static efficiency in these two cases, the efficiency at maximum work (η_{MW}) can not return to the Carnot efficiency (η_C) by taking the heat capacities of the reservoirs to be infinite. The relation between η_C and η_{MW} will be studied in our ongoing work. Besides, the temperature-dependent feature of the reservoir's heat capacity [33], the quantumness of the reservoir [45, 46], and the deviation of entropy production from $1/\tau$ -scaling beyond the slow-driving regime [23, 42, 43, 47] can be taken into consideration.

Acknowledgment.—We thank G. H. Dong and Y. Chen for the helpful suggestions on this manuscript. This work is supported by the National Science Foundation of China (NSFC) (Grants No. 11534002, No. 11875049, No. U1730449, No. U1530401, and No. U1930403), and the National Basic Research Program of China (Grants No. 2016YFA0301201). Y. H. Ma is supported by the China Postdoctoral Science Foundation (Grant No. BX2021030).

-
- [1] K. Huang, *Introduction To Statistical Physics, 2Nd Edition* (T&F/Crc Press, 2013), ISBN 978-1-4200-7902-9.
- [2] B. Andresen, R. S. Berry, M. J. Ondrechen, and P. Salamon, *Acco. Chem. Res.* **17**, 266 (1984).
- [3] U. Seifert, *Rep. Prog. Phys.* **75**, 126001 (2012).
- [4] V. Holubec and A. Ryabov, *Phys. Rev. E* **96** (2017).
- [5] R. Kosloff, *J. Chem. Phys.* **150**, 204105 (2019).
- [6] Z.-C. Tu, *Front. Phys.* **16**, 1 (2021).
- [7] J. Yvon, in *First Geneva Conf. Proc. UN* (1955).
- [8] P. Chambadal, *Recuperation de chaleur a la sortie d' un reacteur, chapter 3* (1957).
- [9] I. I. Novikov, *J. Nucl. Energy II* **7**, 125 (1958).
- [10] F. L. Curzon and B. Ahlborn, *Am. J. Phys.* **43**, 22 (1975).
- [11] C. V. den Broeck, *Phys. Rev. Lett.* **95**, 190602 (2005).
- [12] Y. Izumida and K. Okuda, *EPL* **83**, 60003 (2008).
- [13] T. Schmiedl and U. Seifert, *EPL* **83**, 30005 (2008).
- [14] Z. C. Tu, *Journal Phys. A: Math. Theor.* **41**, 312003 (2008).
- [15] M. Esposito, R. Kawai, K. Lindenberg, and C. V. den Broeck, *Phys. Rev. Lett.* **105**, 150603 (2010).
- [16] Y. Wang and Z. C. Tu, *Phys. Rev. E* **85**, 011127 (2012).
- [17] C. V. D. Broeck, *EPL* **101**, 10006 (2013).
- [18] V. Holubec and A. Ryabov, *Phys. Rev. E* **92**, 052125 (2015).
- [19] V. Holubec and A. Ryabov, *J. Stat. Mech. Theo. Exp.* **2016**, 073204 (2016).
- [20] R. Long and W. Liu, *Phys. Rev. E* **94**, 052114 (2016).
- [21] N. Shiraishi, K. Saito, and H. Tasaki, *Phys. Rev. Lett.* **117**, 190601 (2016).
- [22] V. Cavina, A. Mari, and V. Giovannetti, *Phys. Rev. Lett.* **119**, 050601 (2017).
- [23] Y.-H. Ma, D. Xu, H. Dong, and C.-P. Sun, *Phys. Rev. E* **98**, 042112 (2018).
- [24] A. C. Barato and U. Seifert, *Phys. Rev. Lett.* **114**, 158101 (2015).
- [25] J. M. Horowitz and T. R. Gingrich, *Phys. Rev. E* **96**, 020103(R) (2017).
- [26] M. J. Ondrechen, B. Andresen, M. Mozurkewich, and R. S. Berry, *Am. J. Phys.* **49**, 681 (1981).
- [27] M. J. Ondrechen, M. H. Rubin, and Y. B. Band, *J. Chem. Phys.* **78**, 4721 (1983).
- [28] H. S. Leff, *Am. J. Phys.* **55**, 701 (1987).
- [29] Y. Izumida and K. Okuda, *Phys. Rev. Lett.* **112**, 180603 (2014).
- [30] Y. Wang, *Phys. Rev. E* **90**, 062140 (2014).
- [31] R. S. Johal, *Phys. Rev. E* **94**, 012123 (2016).
- [32] H. Tajima and M. Hayashi, *Phys. Rev. E* **96**, 012128 (2017).
- [33] Y.-H. Ma, *Entropy* **22**, 1002 (2020).
- [34] R. S. Johal and R. Rai, *EPL* **113**, 10006 (2016).
- [35] See Supplemental Materials for detailed discussion on the reversible regime (Sec. I); the lower bound of irreversible entropy production (Sec. II); the dissipation work and power-efficiency trade-off (Sec. III); the bounds of $\tilde{\eta}_{\pm}$ (Sec. IV).
- [36] Y. Izumida and K. Okuda, *Phys. Rev. E* **80**, 021121 (2009).
- [37] K. Proesmans and C. Van den Broeck, *Phys. Rev. Lett.* **115**, 090601 (2015).
- [38] Y. Izumida, *Phys. Rev. E* **103**, L050101 (2021).
- [39] G. Ruppeiner, *Phys. Rev. A* **20**, 1608 (1979).
- [40] P. Salamon and R. S. Berry, *Phys. Rev. Lett.* **51**, 1127 (1983).
- [41] G. E. Crooks, *Phys. Rev. Lett.* **99** (2007).
- [42] Y.-H. Ma, D. Xu, H. Dong, and C.-P. Sun, *Phys. Rev. E* **98**, 022133 (2018).
- [43] Y.-H. Ma, R.-X. Zhai, J. Chen, H. Dong, and C. P. Sun, *Phys. Rev. Lett.* **125**, 210601 (2020).
- [44] I. A. Martínez, É. Roldán, L. Dinis, D. Petrov, J. M. R. Parrondo, and R. A. Rica, *Nat. Phys.* **12**, 67 (2015).
- [45] D. Xu, S.-W. Li, X. Liu, and C. Sun, *Phys. Rev. E* **90**, 062125 (2014).
- [46] J. Roßnagel, O. Abah, F. Schmidt-Kaler, K. Singer, and E. Lutz, *Phys. Rev. Lett.* **112** (2014).
- [47] Y.-H. Ma, H. Dong, and C. P. Sun, arXiv:2012.08748 (2020).

Supplementary Materials for "Optimizing Thermodynamic cycles with Finite-Sized Reservoirs"

Hong Yuan,¹ Yu-Han Ma,^{1,*} and C. P. Sun^{1,2,†}

¹Graduate School of China Academy of Engineering Physics,
No. 10 Xibeiwang East Road, Haidian District, Beijing, 100193, China
²Beijing Computational Science Research Center, Beijing 100193, China

This document is devoted to providing the detailed derivations and the supporting discussions to the main content of the Letter. In Sec. I, we discuss the final uniform temperature \bar{T} , the maximum work W_{\max} , and the corresponding efficiency η_{MW} in the reversible regime under the quasi-static limit. The lower bound of irreversible entropy production, illustrated in [Eq. (5)] of the main text, is derived in Sec. II. In Sec. III, we show the proofs of the lower bound of dissipation work $W_d \geq T_b \Sigma_{\min}/\tau$, and the trade-off between power and efficiency presented in [Eq. (10)] of the main text. The derivation of the bounds for efficiency at arbitrary given power, i.e., $\tilde{\eta}_{\pm}$ [Eq. (11) of the main text], is given in Sec. IV.

I. THE REVERSIBLE REGIME

The extractable work from the reservoirs in the reversible regime, $W_{\max} \equiv \lim_{\sigma \rightarrow 0} W(\tau)$, is the upper bound of the work output until the heat engines stop operating. Such bound is achieved with no irreversible entropy production in the whole process [1-3]. Specifically, in an infinitesimal process, The heat engine absorbs $dQ_h = -C_h \dot{T}_h dt$ from the hot reservoir, and then transforms it into the infinitesimal work the $dW_{\max} = \dot{W}_{\max} dt$ with the corresponding time-dependent Carnot efficiency $\eta_C(t) \equiv 1 - T_c/T_h$ [2]. In this sense, the power of the engine reads

$$\dot{W}_{\max} = \eta_C(t) \dot{Q}_h = -C_h \dot{T}_h \left(1 - \frac{T_c}{T_h}\right). \quad (1)$$

On the other hand, according to the conservation of energy, we can also write

$$\dot{W} = \dot{Q}_h - \dot{Q}_c = -C_h \dot{T}_h - C_c \dot{T}_c, \quad (2)$$

where $\dot{Q}_c = C_c \dot{T}_c$ is the heat flow from the heat engine to the cold reservoir. Comparing Eq. (1) and Eq. (2), one has

$$-C_h \frac{\dot{T}_h}{T_h} = C_c \frac{\dot{T}_c}{T_c}, \quad (3)$$

In the case with constant heat capacity $C_h(C_c)$, by integrating both side of Eq. (3) from the beginning to the end of the whole process, the final uniform temperature of the total system, $T_b \equiv T_c^{(f)} = T_h^{(f)}$, is found as

$$T_b = \left[T_h^{(i)}\right]^{\frac{1}{\gamma+1}} \left[T_c^{(i)}\right]^{\frac{\gamma}{\gamma+1}}, \quad (4)$$

where $\gamma \equiv C_c/C_h$ is defined as the heat capacity ratio. As a consequence, integrating Eq. (2), we have

$$W_{\max} = C_h \left[T_h^{(i)} - T_b\right] - C_c \left[T_b - T_c^{(i)}\right]. \quad (5)$$

The first term of the right hand of Eq. (5) is the reversible heat absorbed, $Q_h(\sigma \rightarrow 0) = C_h \left[T_h^{(i)} - T_b\right]$, achieved in the quasi-static limit. In this case, the corresponding efficiency, namely, the efficiency at maximum work output (EMW) $\eta_{\text{MW}} \equiv W_{\max}/Q_h(\sigma \rightarrow 0)$, is directly obtained as [3]

$$\eta_{\text{MW}} = 1 - \gamma \left[\frac{\eta_C}{1 - (1 - \eta_C)^{\frac{\gamma}{\gamma+1}}} - 1 \right], \quad (6)$$

where $\eta_C \equiv \eta_C(0) = 1 - T_c^{(i)}/T_h^{(i)}$ is the Carnot efficiency determined by the initial temperature of the two reservoirs. As we mentioned before, this result is applicable to the heat reservoirs with constant heat capacity. For the reservoirs with temperature-dependent heat capacity, the generalization of Eq. (6) is studied our previous work [3].

* yhma@g scaep.ac.cn

† suncp@g scaep.ac.cn

II. LOWER BOUND OF IRREVERSIBLE ENTROPY GENERATION

It follows from [Eq. (3)] and [Eq. (4)] the main text that

$$\sigma(\tau) \geq \frac{\left(\int_0^\tau \sqrt{\dot{\sigma}} dt\right)^2}{\tau} = \frac{\left(\int_0^\tau C_h \dot{T}_h / \sqrt{L_{22}} dt\right)^2}{\tau} = \frac{\left(\int_{T_h^{(i)}}^{\tilde{T}} C_h dT_h / \sqrt{L_{22}}\right)^2}{\tau} \equiv \frac{\Sigma}{\tau}, \quad (7)$$

where $\Sigma = \Sigma(\tilde{T})$, and $T_h(\tau) \equiv \tilde{T} = \tilde{T}(\sigma)$ is given by [Eq. (2)] of the main text. In the linear irreversible regime, keeping the first order of σ in $\tilde{T}(\sigma)$, [Eq. (2)] of the main text is approximated as

$$\tilde{T} = T_b \exp\left[\frac{\sigma}{C_h + C_c}\right] \approx T_b \left[1 + \frac{\sigma}{C_h + C_c}\right]. \quad (8)$$

Then, Σ is approximated as

$$\Sigma = \Sigma(\tilde{T} = T_b) + \left.\frac{\partial \Sigma}{\partial \tilde{T}}\right|_{\tilde{T}=T_b} (\tilde{T} - T_b) \quad (9)$$

$$= \left(\int_{T_h^{(i)}}^{T_b} C_h dT_h / \sqrt{L_{22}}\right)^2 + 2 \left(\int_{T_h^{(i)}}^{T_b} C_h dT_h / \sqrt{L_{22}}\right) \frac{\sigma}{\sqrt{L_{22}}(1+\gamma)}, \quad (10)$$

up to the first order of σ . Substituting the above result into Eq. (7), we obtain

$$\sigma = \sigma(\tau) \geq \frac{\Sigma_{\min}}{\tau} \left[1 - \frac{2\sqrt{\Sigma_{\min}/L_{22}}}{(1+\gamma)\tau}\right]^{-1}, \quad (11)$$

where $\Sigma_{\min} \equiv \left(\int_{T_h^{(i)}}^{T_b} C_h dT_h / \sqrt{L_{22}}\right)^2$ is a τ -independent dissipation coefficient. By expanding the right hand of this inequality with respect to τ^{-1} , we have

$$\sigma(\tau) \geq \frac{\Sigma_{\min}}{\tau} \left[1 + \frac{2\sqrt{\Sigma_{\min}/L_{22}}}{(1+\gamma)\tau}\right] + \mathcal{O}(\tau^{-3}). \quad (12)$$

In the long-time regime, up to the first order of τ^{-1} , we obtain [Eq. (5)] of the main text, namely, $\sigma(\tau) \geq \Sigma_{\min}/\tau$. To be consistent with this result, all the high-order terms of τ^{-1} will be ignored in the following discussion.

III. DISSIPATION WORK AND POWER-EFFICIENCY TRADE-OFF

A. The dissipation work

The work output $W(\tau) = Q_h(\tau) - Q_c(\tau)$ is explicitly written as

$$W(\tau) = C_h [T_h^{(i)} - \tilde{T}] - C_c [\tilde{T} - T_c^{(i)}] = C_h T_h^{(i)} + C_c T_c^{(i)} - (C_c + C_h) \tilde{T}, \quad (13)$$

which is monotonically decreasing as \tilde{T} increases. It follows from Eqs. (5) and (13) that the dissipation work reads

$$W_d(\tau) = W_{\max} - W(\tau) = (C_c + C_h) (\tilde{T} - T_b). \quad (14)$$

Combining [Eq. (2)] and [Eq. (5)] of the main text, one has

$$\tilde{T} \geq T_b \exp \left[\frac{\Sigma_{\min}}{(C_c + C_h)\tau} \right], \quad (15)$$

and then Eq. (14) is written in terms of τ as,

$$W_d(\tau) \geq (C_h + C_c) T_b \left[e^{\frac{\Sigma_{\min}}{(C_c + C_h)\tau}} - 1 \right] = \frac{T_b \Sigma_{\min}}{\tau} + \mathcal{O}(\tau^{-2}). \quad (16)$$

Up to the first order of τ^{-1} , the inequality for the dissipation work in main text is obtained as $W_d(\tau) \geq T_b \Sigma_{\min}/\tau$.

B. Power-efficiency trade-off

As shown in [Eq. (9)] of the main text that

$$\frac{\eta_{\text{MW}} - \eta}{\eta_{\text{MW}} [1 - \eta/(1 + \gamma)]} \geq \frac{T_b \Sigma_{\min}}{W_{\max} \tau}, \quad (17)$$

which becomes, by multiplying both sides by $W(\tau)$,

$$\frac{W(\tau) (\eta_{\text{MW}} - \eta)}{\eta_{\text{MW}} [1 - \eta/(1 + \gamma)]} \geq \frac{T_b \Sigma_{\min} W(\tau)}{W_{\max} \tau} = \frac{T_b \Sigma_{\min} P}{W_{\max}}. \quad (18)$$

Here, $P \equiv W(\tau)/\tau$ is defined as the average power of the whole process. Further, we rewrite $W(\tau)$ as

$$W(\tau) = W_{\max} - W_d = W_{\max} - \frac{W_{\max} (\eta_{\text{MW}} - \eta)}{\eta_{\text{MW}} [1 - \eta/(1 + \gamma)]}, \quad (19)$$

then Eq. (18) becomes

$$W_{\max} \left\{ 1 - \frac{\eta_{\text{MW}} - \eta}{\eta_{\text{MW}} [1 - \eta/(1 + \gamma)]} \right\} \frac{(\eta_{\text{MW}} - \eta)}{\eta_{\text{MW}} [1 - \eta/(1 + \gamma)]} \geq \frac{T_b \Sigma_{\min} P}{W_{\max}}. \quad (20)$$

By straightforward calculation, the above inequality is simplified as

$$P \leq \frac{W_{\max}^2}{\eta_{\text{MW}}^2 T_b \Sigma_{\min}} \frac{\eta [1 - \eta_{\text{MW}}/(1 + \gamma)] (\eta_{\text{MW}} - \eta)}{[1 - \eta/(1 + \gamma)]^2}. \quad (21)$$

On the other hand, the average power follows

$$P = \frac{W(\tau)}{\tau} = \frac{W_{\max} - W_d}{\tau} \leq \frac{W_{\max} - T_b \Sigma_{\min}/\tau}{\tau}, \quad (22)$$

where $W_d \geq T_b \Sigma_{\min}/\tau$ has been used. The above relation can be further written in the quadratic form, namely,

$$P \leq -T_b \Sigma_{\min} \left(\frac{1}{\tau} - \frac{W_{\max}}{2T_b \Sigma_{\min}} \right)^2 + \frac{W_{\max}^2}{4T_b \Sigma_{\min}}, \quad (23)$$

which clearly shows that the maximum average power and the corresponding optimal operation time are

$$P = \frac{W_{\max}^2}{4T_b \Sigma_{\min}} \equiv P_{\max}, \text{ and } \tau = \frac{2T_b \Sigma_{\min}}{W_{\max}} \equiv \tau^*, \quad (24)$$

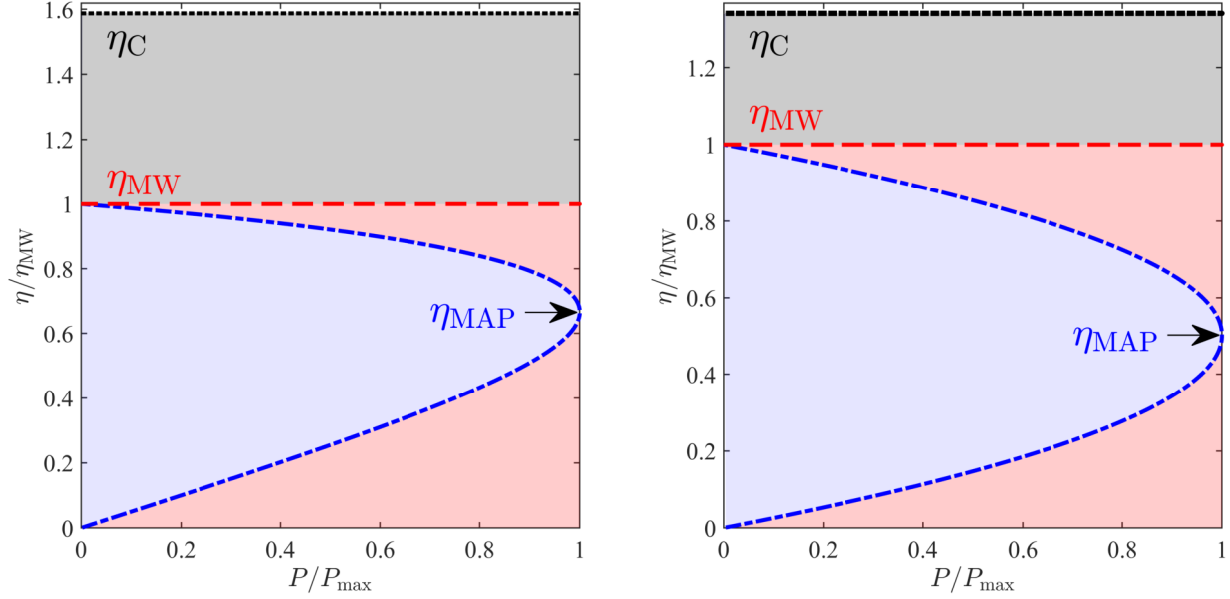


Figure 1. "Phase diagram" $\tilde{P} - \tilde{\eta}$ of the heat engine performance between finite reservoirs with different heat capacity ratio $\gamma = C_c/C_h$. Here, $\gamma = 0.01$ for the left plot and $\gamma = 100$ for the right plot. The blue dash-dotted curve and the (light blue) area therein represent the trade-off between $\tilde{P} = P/P_{\max}$ and $\tilde{\eta} = \eta/\eta_{\text{MW}}$ in Eq. (26), where P_{\max} is the maximum average power. The efficiency at maximum work η_{MW} in Eq. (6) is plotted with the red dashed line, while the corresponding Carnot efficiency $\eta_C = 0.8$ is plotted with the black dotted line.

respectively. Finally, with the definitions

$$\tilde{P} \equiv \frac{P}{P_{\max}}, \tilde{\eta} \equiv \frac{\eta}{\eta_{\text{MW}}}, \lambda \equiv 1 - \frac{\eta_{\text{MW}}}{1 + \gamma}, \quad (25)$$

Eq. (21) is re-expressed as a concise form

$$\tilde{P} \leq \frac{4\lambda\tilde{\eta}(1 - \tilde{\eta})}{(\lambda\tilde{\eta} + 1 - \tilde{\eta})^2}. \quad (26)$$

This is the trade-off between power and efficiency as we presented in [Eq. (10)] of the main text. In [Fig. 2] of the main text, we plot such trade-off in the symmetric case with $\gamma = 1$. As comparisons, the trade-off in the asymmetric cases with $\gamma = 0.01, 100$ are shown in Fig. 1.

IV. BOUNDS OF EFFICIENCY AT ARBITRARY GIVEN POWER

Note that the numerator in the right side of the trade-off in Eq. (26) can be re-expressed as

$$4\lambda\tilde{\eta}(1 - \tilde{\eta}) = (\lambda\tilde{\eta} + 1 - \tilde{\eta})^2 - [\lambda\tilde{\eta} - (1 - \tilde{\eta})]^2. \quad (27)$$

Thus, the trade-off is re-written as

$$\tilde{P} + \left[\frac{\lambda\tilde{\eta} - (1 - \tilde{\eta})}{\lambda\tilde{\eta} + 1 - \tilde{\eta}} \right]^2 \leq 1. \quad (28)$$

Such that, the upper and lower bounds in $\tilde{\eta}_- \leq \tilde{\eta} \leq \tilde{\eta}_+$ are the solutions of the quadratic equation

$$\left[\frac{\lambda\tilde{\eta} - (1 - \tilde{\eta})}{\lambda\tilde{\eta} + 1 - \tilde{\eta}} \right]^2 = 1 - \tilde{P}. \quad (29)$$

By straightforward calculation, one has

$$\tilde{\eta}_{\pm} = \frac{1 \pm \sqrt{1 - \tilde{P}}}{1 \pm \sqrt{1 - \tilde{P}} + \lambda(1 \mp \sqrt{1 - \tilde{P}})} = 1 - \frac{\lambda(1 \mp \sqrt{1 - \tilde{P}})}{1 \pm \sqrt{1 - \tilde{P}} + \lambda(1 \mp \sqrt{1 - \tilde{P}})}. \quad (30)$$

With the help of the relation

$$\tilde{P} = 1 - (\sqrt{1 - \tilde{P}})^2 = (1 \mp \sqrt{1 - \tilde{P}})(1 \pm \sqrt{1 - \tilde{P}}), \quad (31)$$

Eq. (30) is simplified as

$$\tilde{\eta}_{\pm} = 1 - \frac{\lambda\tilde{P}}{(1 \pm \sqrt{1 - \tilde{P}})^2 + \lambda\tilde{P}}. \quad (32)$$

This is the result we presented in [Eq. (11)] of the main text.

-
- [1] M. J. Ondrechen, B. Andresen, M. Mozurkewich, and R. S. Berry, *Am. J. Phys.* **49**, 681 (1981).
 [2] Y. Izumida and K. Okuda, *Phys. Rev. Lett.* **112**, 180603 (2014).
 [3] Y.-H. Ma, *Entropy* **22**, 1002 (2020).